

# **Chapter 5**

---

---

## **Results and Discussion**

---

---

## 5.1 Introduction

This chapter focuses on medium frequency range horizontal mechanical vibration on the die-cast A308 aluminium alloy to increase nucleation sites during melt solidification by fragmenting dendrites and Si particles with the turbulence created by the mechanical vibration. The performance of the as-cast and vibrated cast samples was addressed in terms of metallurgical, physical, and mechanical features. Hence keeping that in mind, the chapter has been divided into four sections (a) Microstructural observation, (b) Density and porosity evaluation, (c) Mechanical properties, and (d) Fractography. The chapter concludes with a summary of the microstructure, physical, and mechanical results.

## 5.2 Effects of medium frequency range horizontal mechanical vibration on the metallurgical, physical, and mechanical properties of cast A308 alloy

This study investigated the microstructure, physical, and mechanical properties of die-cast A308 alloy subjected to mechanical vibration during solidification. Different frequencies (0, 20, 30, 40, and 50 Hz) at constant amplitude (31  $\mu\text{m}$ ) were employed using a power amplifier as the power input device. X-ray diffraction, optical microscopy, and scanning electron microscopy were used to examine the morphological changes in the cast samples under stationary and vibratory conditions. Metallurgical features of the castings were evaluated using ImageJ software. The average values of metallurgical characteristics, including primary  $\alpha$ -Al grain size, dendrite arm spacing, the average area of eutectic silicon, aspect ratio, and percentage porosity, were reduced by 34%, 59%, 56%, 22%, and 62%, respectively, at 30 Hz frequency compared with stationary casting. Mechanical tests of the cast samples showed that the yield strength (YS), ultimate tensile strength (UTS), percentage elongation (%EL), and microhardness (HV) increased by 8%,

13%, 17%, and 16%, respectively, at 30 Hz frequency compared with stationary casting. The fractured surface of the tensile specimens exhibited mixed-mode fracture behaviour because of brittle facets, cleavage facets, ductile tearing, and dimple morphologies. The presence of small dimples showed that plastic deformation occurred before fracture.

### **5.3 Results and discussion**

#### **5.3.1 Microstructural observation**

The optical micrographs of the cast A308 aluminium alloys under mechanical vibration at different frequencies (0, 20, 30, 40, and 50 Hz) and constant amplitude (31  $\mu\text{m}$ ) are presented in Fig. 5.1. The corresponding SEM micrographs are shown in Figure 5.2. In stationary castings, the eutectic silicon phases are coarse and acicular in size and shape, as shown in Fig. 5.1(a). In stationary castings (0 Hz), the morphology in Fig. 5.1(a) shows the non-uniform distribution of the primary  $\alpha$ -Al phase with coarse dendritic structure and shrinkage porosity. However, the size of primary  $\alpha$ -Al phase grains reduced with some residue dendrites after applying low-frequency (20 Hz) vibration, as shown in Fig. 5.1(b). When the vibration frequency was increased up to 30 Hz, the primary  $\alpha$ -Al phase grains transformed into refined equiaxed grains, and the coarse dendrites disappeared, as shown in Fig. 5.1(c).

When the vibration frequency was increased beyond 30 Hz, the size of the primary  $\alpha$ -Al grains slightly increased. This result may be attributed to the decreased effect of vibration and high forced convection, which increases turbulence [46, 81]. However, no significant effect was observed at 40 and 50 Hz frequencies. The sizes of primary  $\alpha$ -Al grains and eutectic silicon phases slightly increased, as shown in Fig. 5.1 (d) and (e). During solidification, the microstructural changes mainly depended on the cooling rate, which led to the structural grain refinement in the casting [93, 94]. The

cooling rate was maximum at 30 Hz frequency and showed significant improvement in the microstructure.

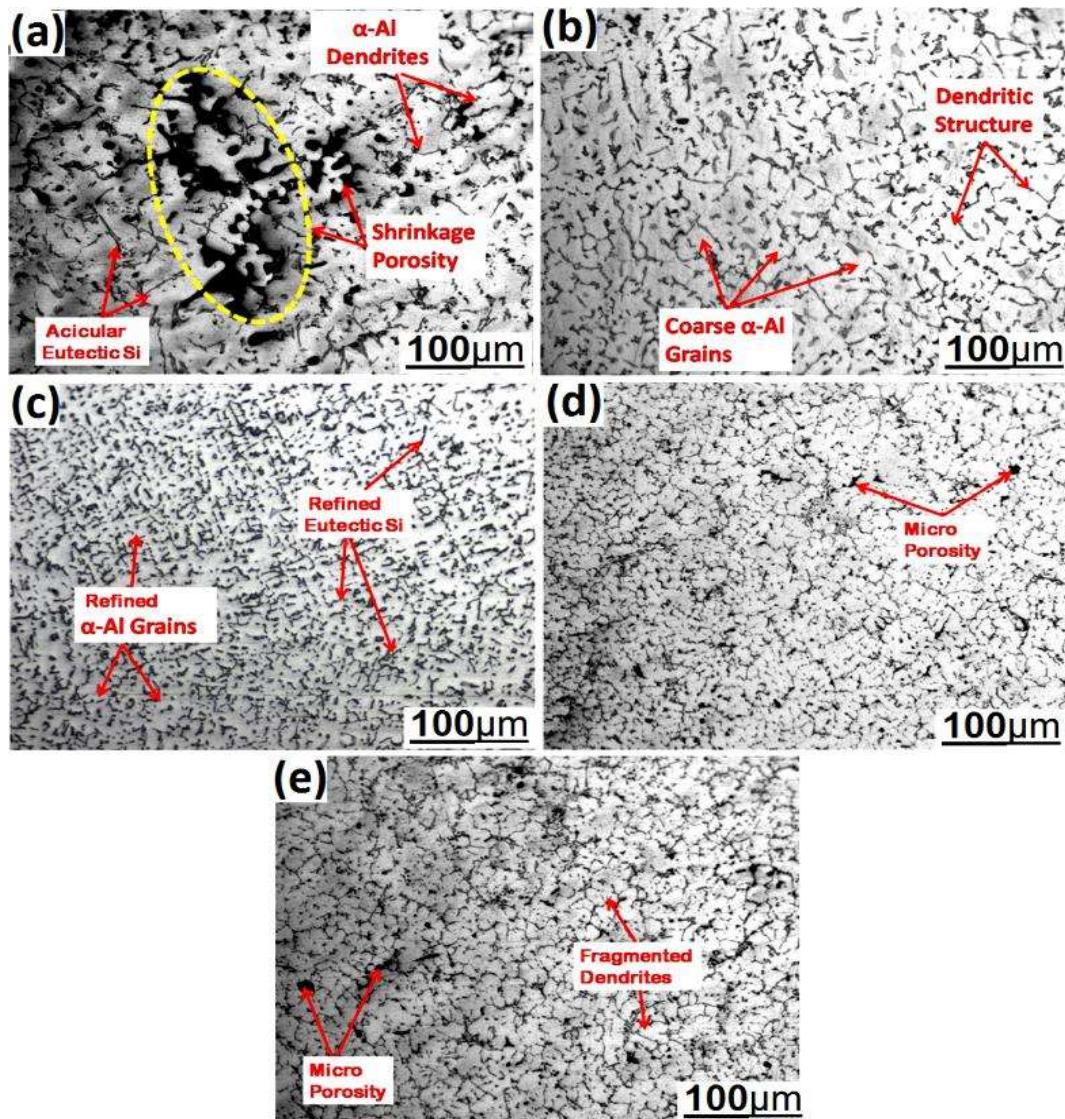


**Figure 5.1:** Optical micrographs of A308 alloys cast under (a) 0 Hz; (b) 20 Hz; (c) 30 Hz; (d) 40 Hz; (e) 50 Hz frequencies.

Quantitative measured values of metallurgical features, such as eutectic silicon properties, DAS, primary  $\alpha$ -Al grain size, and porosity, of the cast A308 aluminium alloy are listed in Tables 5.3 and 5.4. Graphs between the aforementioned metallurgical features are plotted in Fig. 5.3 to show the variation in the microstructures of castings. The obtained results showed that remarkable improvement was achieved at 30 Hz frequency.

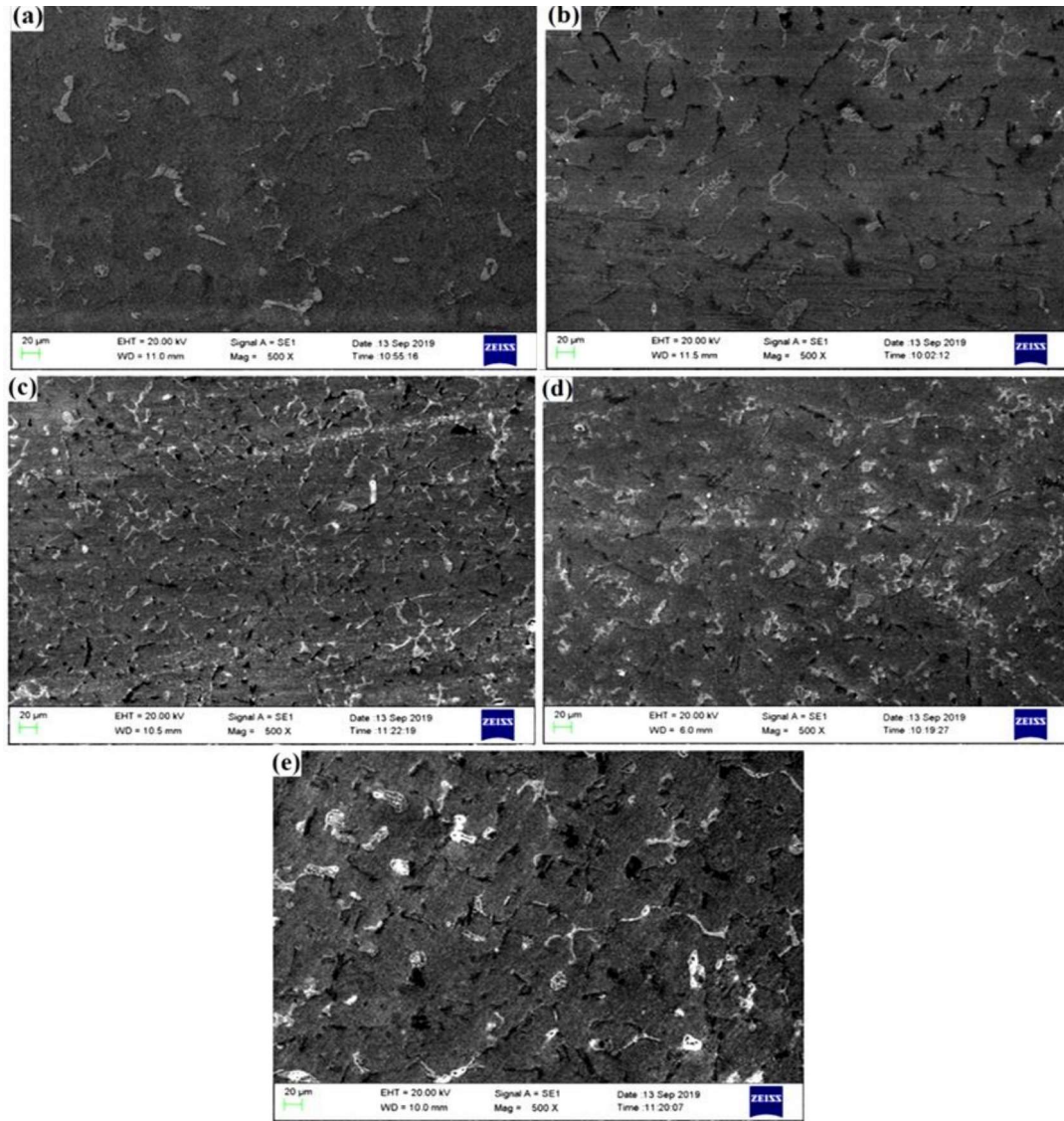


**Figure 5.2:** SEM micrographs of A308 alloys cast under different frequencies: (a) 0 Hz; (b) 20 Hz; (c) 30 Hz; (d) 40 Hz; (e) 50 Hz frequencies.

**Table 5.1:** The cooling rate of casting at (0-50) Hz frequencies

| Frequency /<br>Hz | Temperature / °C |          | Solidification<br>time / s | Cooling rate / (°C·s <sup>-1</sup> ) |
|-------------------|------------------|----------|----------------------------|--------------------------------------|
|                   | Pouring          | Freezing |                            |                                      |
| 0                 | 710              | 520      | 120                        | 1.58                                 |
| 20                | 710              | 520      | 110                        | 1.72                                 |
| 30                | 710              | 520      | 105                        | 1.80                                 |
| 40                | 710              | 520      | 112                        | 1.69                                 |
| 50                | 710              | 520      | 114                        | 1.66                                 |

Metallurgical features, such as average values of primary  $\alpha$ -Al grain size, DAS, the average area of eutectic silicon, aspect ratio, and % porosity, were reduced by 34%, 59%, 56%, 22%, and 62%, respectively. However, the average percentage roundness and average shape factor of the eutectic silicon phases increased by 25% and 193%, respectively, at 30 Hz frequency compared to stationary casting. Their value decreased slightly when the frequency was further increased, as shown in Fig. 5.3(b). Such improvement may be attributed to the fragmentation of dendrites and the generation of new nucleation sites, which promote grain refinements during solidification under optimum mould vibration [48, 56, 77, 95]

**Table 5.2:** Morphological features of eutectic silicon particles at (0-50) Hz frequencies

| Frequency / Hz | Average aspect ratio<br>$= d_{\min}/d_{\max}$ | Average shape factor<br>(SF) = $4\pi A/P^2$ | Average area of eutectic Si / $\mu\text{m}^2$ | Average roundness / % |
|----------------|---|---|---|-----------------------|
| 0              | 2.37  | 0.0850                                      | 602.64  | 46                    |
| 20             | 1.88  | 0.1403                                      | 502.65  | 60                    |
| 30             | 1.85  | 0.2497                                      | 261.71  | 61                    |
| 40             | 2.09  | 0.1965                                      | 416.73  | 55                    |
| 50             | 1.98  | 0.1499                                      | 462.34  | 53                    |

Notes:  $d_{\min}$  is the minimum diameter;  $d_{\max}$  is the maximum diameter;  $A$  denotes area;  $P$  denotes perimeter.

**Table 5.3:** Average  $\alpha$ -Al grain size, dendrite arm spacing (DAS), and porosity of A308 Al-alloy under (0-50) Hz frequencies

| Frequency / Hz | Average $\alpha$ -Al grain size / $\mu\text{m}$ | DAS / $\mu\text{m}$ | Porosity / % |
|----------------|---|---------------------|--------------|
| 0              | 82.65   | 69.71               | 2.33         |
| 20             | 66.94   | 48.75               | 1.61         |
| 30             | 54.31   | 28.31               | 0.89         |
| 40             | 55.79   | 33.59               | 1.25         |
| 50             | 61.53   | 48.29               | 1.96         |

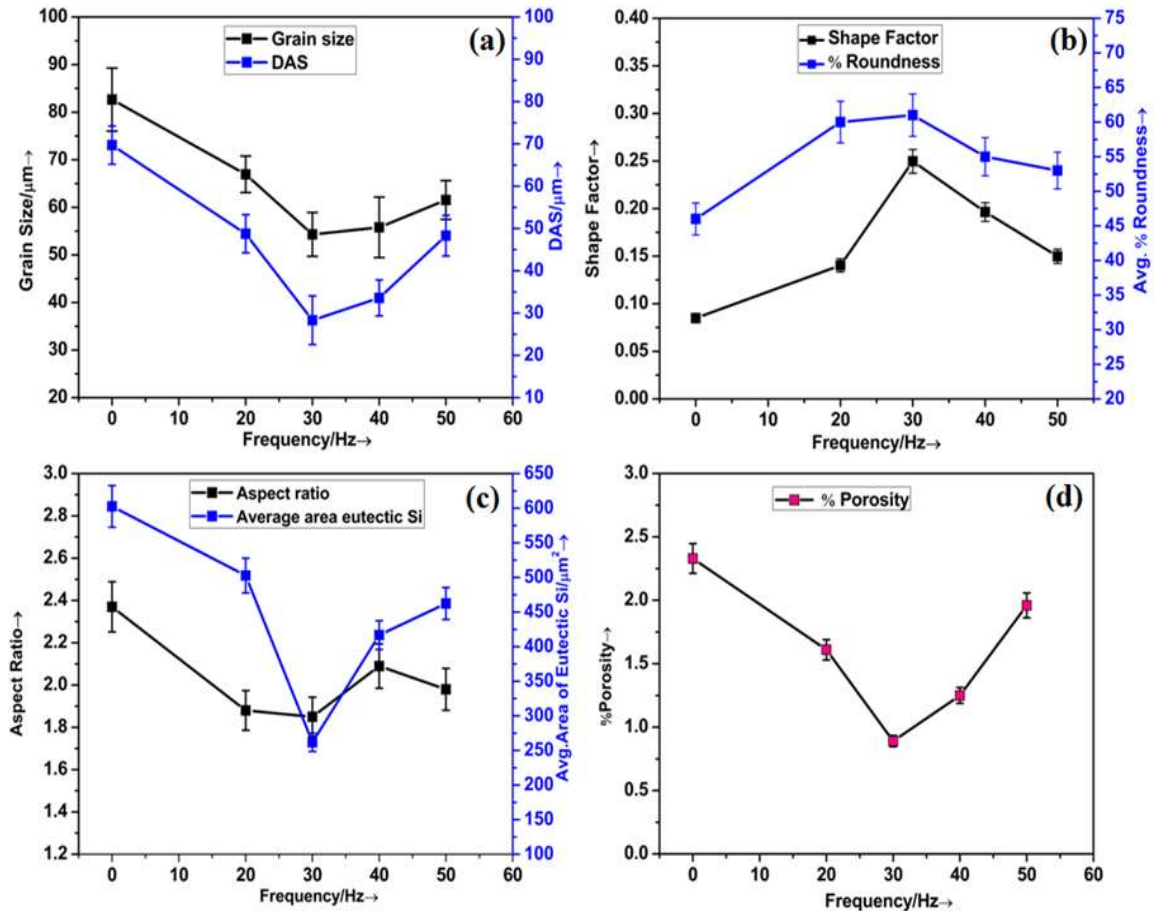


**Figure 5.3:** Comparative study of microstructural features of A308 alloy cast under stationary and vibratory conditions: (a) grain size and DAS; (b) shape factor and average roundness; (c) aspect ratio and average area of eutectic Si; (d) porosity.

### 5.3.2 X-ray diffraction and SEM-EDS analysis

The  $\alpha$ -Al,  $\text{Al}_2\text{Cu}$ ,  $\text{Fe}_{1.7}\text{SiAl}_4$ , and eutectic silicon were confirmed from the XRD analysis data using JCPDS-ISDD 2003 software, as shown in Fig. 5.4. The elements found in XRD analysis are Al, Si, Cu, and Fe. The possible intermetallic phases are  $\text{Al}_2\text{Cu}$ , and  $\text{Fe}_{1.7}\text{SiAl}_4$ , which can also be observed in the SEM microstructure, as shown in Fig. 5.5(a).

SEM-EDS analysis was carried out to confirm the presence of Al-Fe-Si phases, Al-Si eutectic,  $\text{Al}_2\text{Cu}$ , and Si particles in A308 alloy casting. The cast specimen at 30 Hz frequency was analyzed, and the corresponding EDS spectra of the  $\text{Al}_2\text{Cu}$ , Al-Fe-Si, Al-Si, and Si particles are shown in Figs. 5.5(a-e).

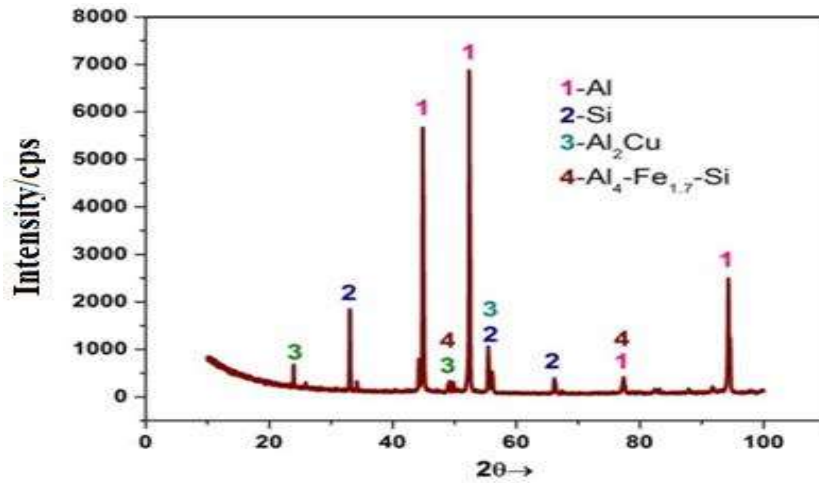


Figure 5.4: X-ray diffraction pattern of A308 alloy.

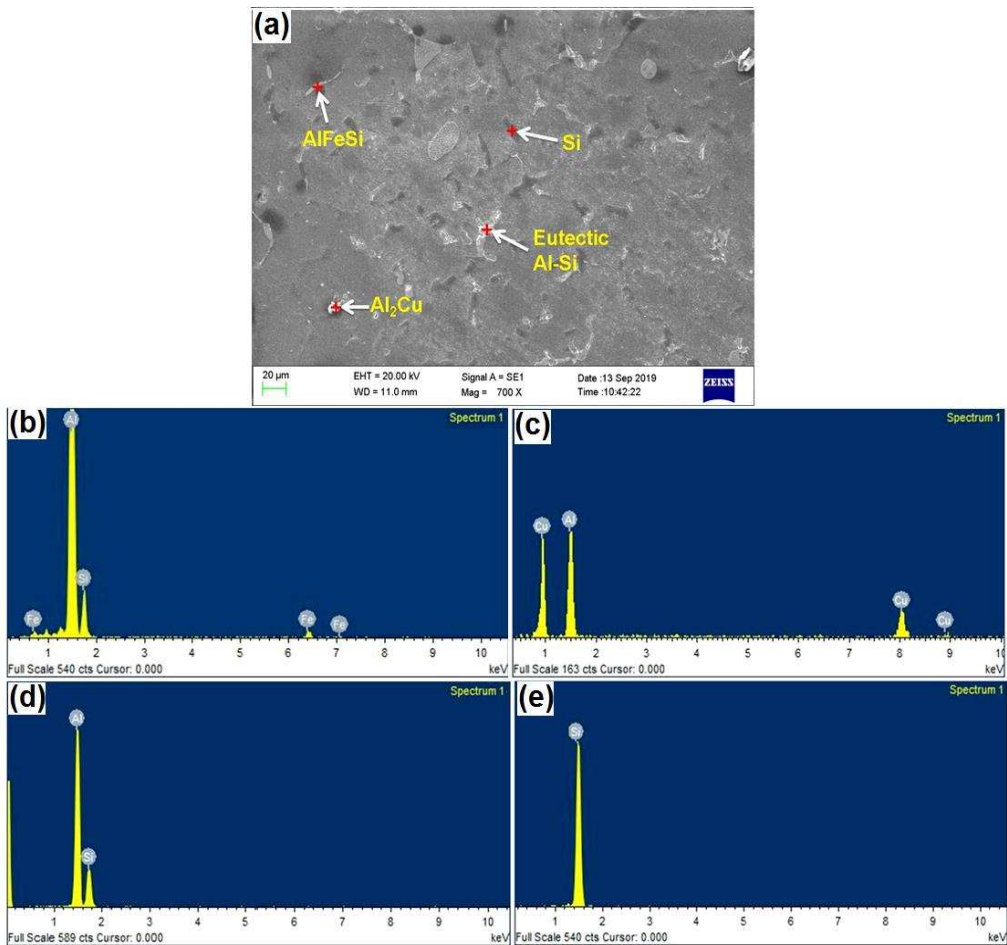


Figure 5.5: SEM image of (a) EDS spectrum of A308 alloy (b) Al-Fe-Si, (c) Al<sub>2</sub>Cu, (d) Al-Si, and (e) Si intermetallic phases.

#### 5.4 Density and porosity analysis

The theoretical density of the A308 alloy and the experimental density of all castings under stationary and vibratory conditions are shown in Table 5.4. The theoretically calculated density of A308 alloy is  $2.795 \text{ g/cm}^3$  (Table 5.4). The calculated values of experimental densities with and without vibrational frequency were compared. The density of the cast sample under the stationary condition was  $2.730 \text{ g/cm}^3$ , which is the least among all the measured values because of the presence of microvoids and shrinkage porosities in interdendritic regions, as shown in Fig. 5.6(a).

**Table 5.4:** Density measurement of A308 alloy under (0-50) Hz frequencies

| Frequency /<br>Hz | Experimental density measurements |                        |  |                       | Theoretical<br>density /<br>( $\text{g}\cdot\text{cm}^3$ ) |
|-------------------|-----------------------------------|------------------------|--|-----------------------|--|
|                   | Weight<br>in air / g              | Weight in<br>water / g | Average<br>density /<br>( $\text{g}\cdot\text{cm}^3$ ) | Standard<br>deviation |  |
| 0                 | 15.060                            | 9.550                  | 2.730  | 0.0031                |  |
| 20                | 14.672                            | 9.366                  | 2.754  | 0.0085                |  |
| 30                | 15.820                            | 10.118                 | 2.775  | 0.0146                | 2.795  |
| 40                | 15.285                            | 9.721                  | 2.764  | 0.0176                |  |
| 50                | 14.446                            | 9.234                  | 2.746  | 0.0207                |  |

By contrast, the porosity gradually reduced, as shown in Fig. 5.6(b) and (c). Consequently, the density increased with increasing frequency up to 30 Hz. The maximum density of cast alloy was  $2.775 \text{ g/cm}^3$  at 30 Hz frequency, which shows a 1.5% improvement in density than that under the stationary condition. This improvement in density was attributed to the increased feeding capacity of the molten metal and improved filling ability under moderate mechanical vibration [8, 47, 96]. However, further increasing the frequency beyond 30 Hz decreased the density of the cast alloy because of turbulences and gas entrapments [81].

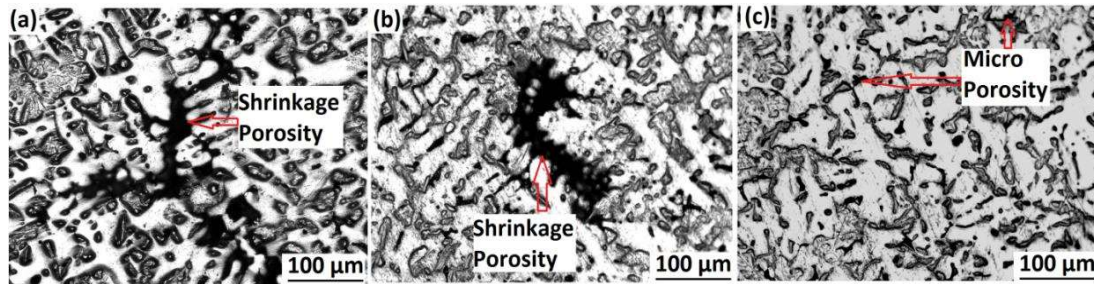


**Figure 5.6:** Interdendritic porosity of as-cast samples: (a) shrinkage porosity at 0 Hz; (b) shrinkage porosity at 20 Hz; (c) available microporosity under vibration at 30 Hz.

## 5.5 Mechanical properties

### 5.5.1 Tensile Properties

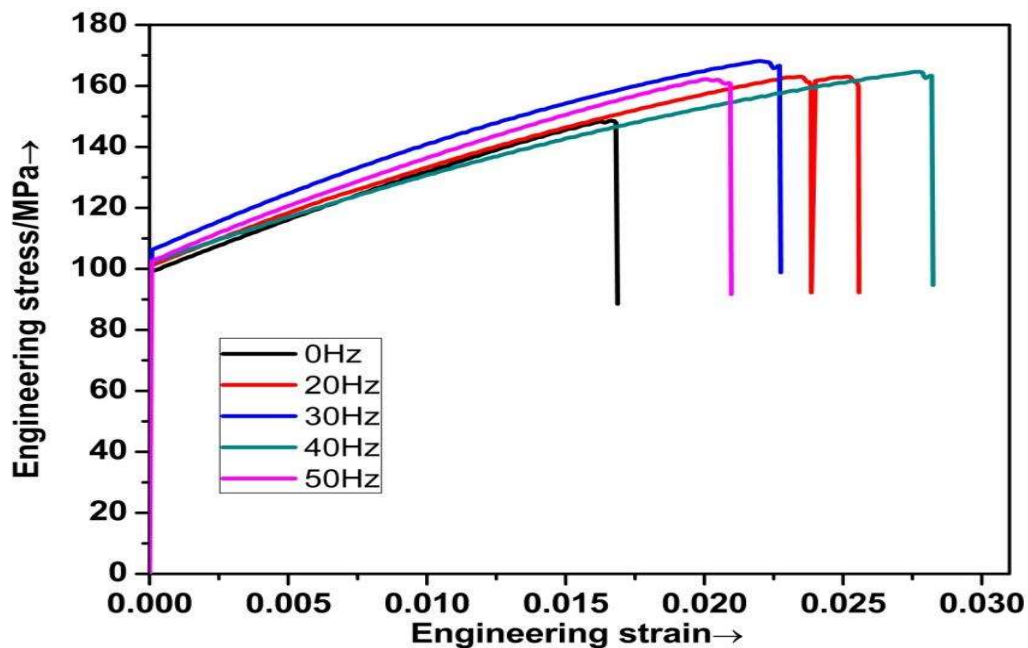


**Figure 5.7:** Engineering stress-strain diagram of tensile test samples at (0-50) Hz frequencies

In this section, the influence of horizontal vibration frequencies on mechanical properties, such as yield strength (YS), ultimate tensile strength (UTS), percentage elongation (%EL), and microhardness (HV), of the cast A308 aluminium alloy under stationary and vibratory conditions was examined. The obtained results are summarized in Figs. 5.7 and 5.8. Fig. 5.7 shows the engineering stress-strain diagram of the cast A308 aluminium alloy under stationary and vibratory conditions. Fig. 5.8 indicates that the cast

specimen under a mechanical vibration at 30 Hz frequency demonstrated the highest tensile strength. The mechanical properties (i.e., YS, UTS %El, and HV) of the castings were improved by 8%, 13%, 17%, and 16%, respectively, at 30 Hz frequency compared with stationary casting due to microstructural refinement ( $\alpha$ -Al size, DAS, and change in morphology of the eutectic silicon [40, 63, 97]. In contrast, the effect of mechanical vibration on the microstructure decreased beyond 30 Hz [81].

### **5.5.2 Microhardness**

The microhardness values of the produced castings under stationary and vibratory conditions were measured using a Vickers hardness tester at 10 N load. A minimum hardness of HV ~74 was observed under the stationary condition for the as-cast A308 aluminium alloy, which can be ascribed to its larger  $\alpha$ -Al grain size, coarse eutectic silicon phases, and larger inter-dendritic shrinkage porosity than the other specimens. Similar to UTS, HV values increased up to 30 Hz frequency and decreased beyond that. When the frequency was increased to 30 Hz, the refined eutectic silicon and intermetallic phases, including  $\text{Al}_2\text{Cu}$  and  $\text{Fe}_{1.7}\text{SiAl}_4$ , dispersed uniformly in the melt because of the convection effect, and significant improvement in microhardness was achieved. The maximum microhardness of HV 86 was achieved at 30 Hz frequency, which shows a 17% improvement. The microhardness value increased because of the refinement of  $\alpha$ -Al grains attributed to the high cooling rate of liquid metal during mechanical vibration [85, 93, 94].

Comparison results of the mechanical properties of the cast A308 aluminium alloy produced under different mechanical vibration conditions are presented in Fig. 5.8. Results showed that the mechanical vibration applied during melting improved the mechanical properties up to a frequency of 30 Hz, after which a slight decrease was observed. Thus, the optimum tensile strength and microhardness values were achieved at

30 Hz frequency, which may be attributed to  $\alpha$ -Al grain refinement and change in morphology of the eutectic silicon [40, 63, 97]. Further increasing the frequency to 40 and 50 Hz led to an increase in  $\alpha$ -Al grain size because of the turbulence of molten alloy under high frequency and caused a slight decrease in the mechanical properties.

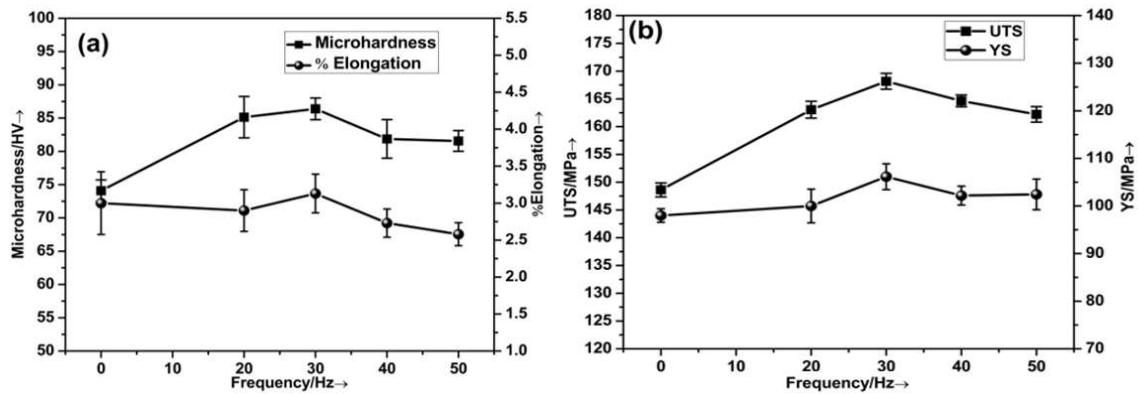


**Figure 5.8:** Comparison of mechanical properties under stationary versus vibratory conditions: (a) microhardness and elongation; (b) UTS and YS.

## 5.6 Fractography

Tensile fractured surfaces of the A308 alloy cast under vibratory conditions were examined using scanning electron microscopy, and the micrographs in Figs. 5.9(a–e) shows the different morphologies of tensile fractured surfaces. As shown in Fig. 5.9(a) and (b), a grape-like dendritic morphology and shrinkage porosity were observed on the fractured surfaces under vibration at low frequencies (0–20 Hz). This result may be attributed to the deterioration in the mechanical strength of the alloys. Most of the fractured surfaces showed a brittle fracture-like appearance, such as brittle facets in Fig. 5.9(b) and (d) and cleavage facets in Fig. 5.9(c).

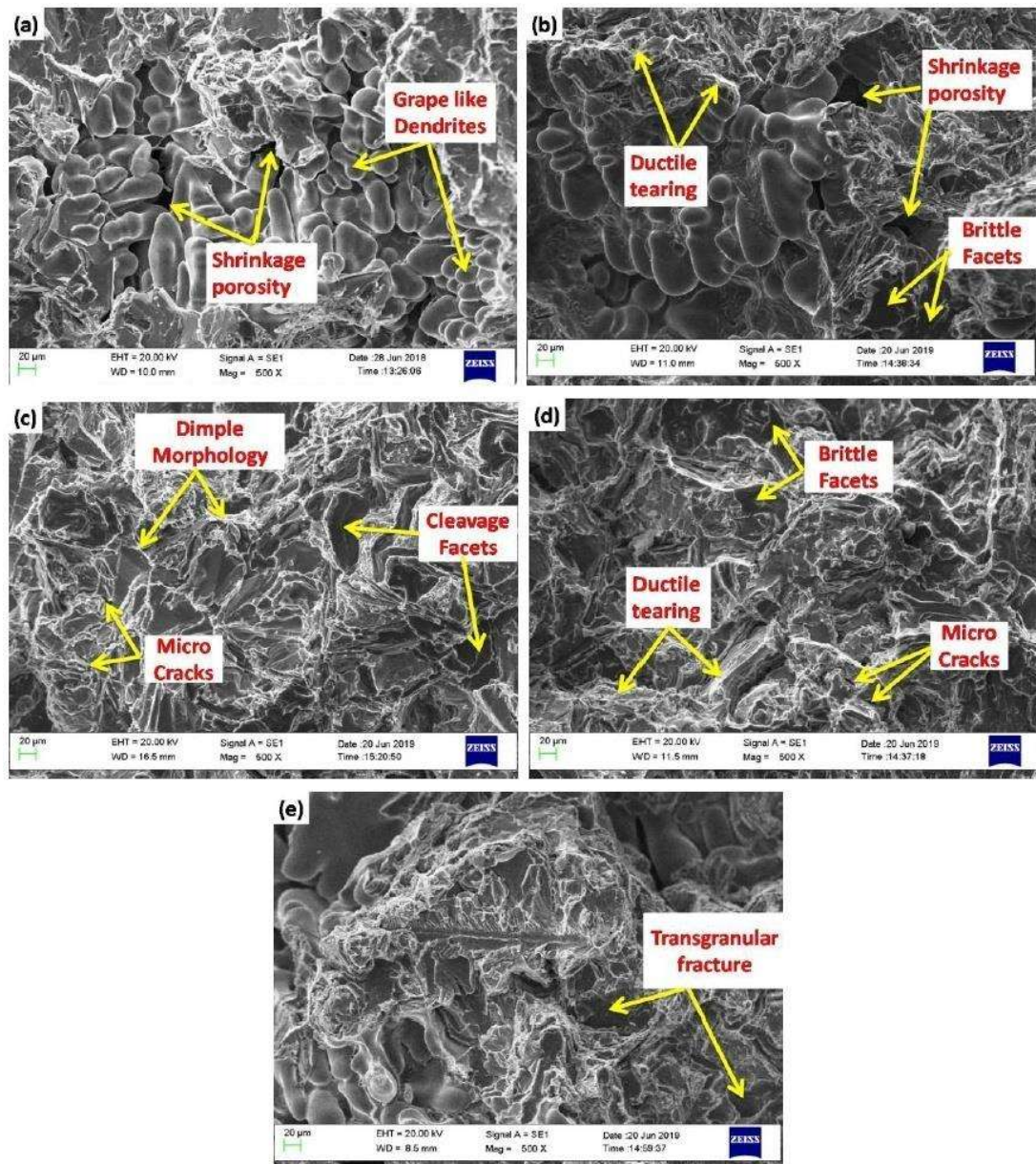


**Figure 5.9:** Fractographs of tensile test specimens at (a) 0 Hz, (b) 20 Hz, (c) 30 Hz, (d) 40 Hz, and (e) 50 Hz frequencies.

The tensile fractured surface showed a transgranular brittle fracture and cleavage facets, as apparent in Fig. 5.9(e). In brittle fracture mode, the cleavage and brittle facet-like morphologies were obvious, but ductile tearing also occurred throughout the fracture surfaces, as shown in Figs. 5.9(a–e). The fractured surface in Fig. 5.9(c) shows that the cleavage facets may be attributed to the hard intermetallic phases, such as  $Al_2Cu$  and  $Al-$

Fe–Si. The fractured surfaces also show some micro-cracks and small voids, which might reduce the density of the alloy and cause the deterioration in mechanical properties. Fig. 5.9(c) shows the dimple-like morphology, which indicates that plastic deformation occurred before fracture. Ductile tearing also occurred, and cleavage facets exhibited mixed-mode fracture behaviour.

## 5.7 Summary

This study investigated the effects of horizontal mechanical vibration on the microstructure, mechanical properties, and fracture behaviour of A308 aluminium alloy. The following conclusions have been drawn.

- (1) Metallurgical features, such as average values of primary  $\alpha$ -Al grain size, DAS, the average area of eutectic silicon, aspect ratio, and porosity, were reduced by 34%, 59%, 56%, 22%, and 62%, respectively. However, the average percentage roundness and average shape factor of eutectic silicon phases increased by 25% and 193%, respectively, at 30 Hz frequency compared with stationary casting.
- (2) The mechanical properties, such as yield strength (YS), ultimate tensile strength (UTS), percentage elongation (%EL), and microhardness (HV) increased by 8%, 13%, 17%, and 16%, respectively, at 30 Hz frequency as compared with stationary casting.
- (3) The tensile test fracture surface of the A308 aluminium alloy at the stationary casting condition showed grape-like dendrites with large shrinkage porosity.
- (4) The fractographs of the A308 aluminium alloy cast under mechanical vibration showed mixed-mode fracture behaviour because of the appearance of brittle facets, ductile tearing, cleavage facets, and dimple morphologies.